NRL Release Number 08-1226-3956

NANO LETTERS

2008
Vol. 8, No. 10
3441-3445

Wafer-scale Reduced Graphene Oxide Films for Nanomechanical Devices

Jeremy T. Robinson,*,† Maxim Zalalutdinov,‡ Jeffrey W. Baldwin,† Eric S. Snow,† Zhongqing Wei,† Paul Sheehan,† and Brian H. Houston†

Naval Research Laboratory, Washington, D.C. 20375, and SFA Inc., Crofton, Maryland 21114

Received July 30, 2008; Revised Manuscript Received August 10, 2008

ABSTRACT

We report a process to form large-area, few-monolayer graphene oxide films and then recover the outstanding mechanical properties found in graphene to fabricate high Young's modulus (<*E*> = 185 GPa), low-density nanomechanical resonators. Wafer-scale films as thin as 4 nm are sufficiently robust that they can be delaminated intact and resuspended on a bed of pillars or field of holes. From these films, we demonstrate radio frequency resonators with quality factors (up to 4000) and figures of merit ($f \times Q > 10^{11}$) well exceeding those of pure graphene resonators reported to date. These films' ability to withstand high in-plane tension (up to 5 N/m) as well as their high *Q*-values reveals that film integrity is enhanced by platelet-platelet bonding unavailable in pure graphite.

Nanoelectromechanical systems (NEMS) are an exciting frontier[1] for the next generation devices in both sensing[2−4] and computing.[5] As NEMS resonators shrink below 100 nm they begin to achieve high operating frequencies (up to 10^9 Hz) with extreme sensitivities. At present, high-frequency NEMS are primarily based upon high-modulus materials (>∼100 GPa) such as Si and GaAs that are also relatively easy to process into complex planar structures. For any NEMS system, the most important material properties are the Young's modulus, E, and density, ρ, which dictate the speed of sound in the material, c, and fundamental frequency (f_o) of the device with $f_o \propto c = (E/\rho)^{1/2}$. Of the many materials one might choose, carbon, in the form of diamond, carbon nanotubes, or graphene, exhibits the highest E/ρ ratios, and graphene in particular is most intriguing as it is composed of a single atomic sheet of sp^2-bonded carbon. Atomically thin graphene resonators have recently been demonstrated on small scales and have shown extremely high stiffness to weight ratios.[6,7]

Accessing the superlative properties of graphene-based materials has been frustrated by the difficulty[8] of forming and manipulating large-area, ultrathin films. Current techniques such as mechanical exfoliation[9,10] or growth on SiC[11] are not amenable to fabrication. Mechanical exfoliation is insufficiently reproducible while SiC growth substrates are prohibitively expensive. Techniques are now emerging to address this challenge[12−15] many of which are based on graphite oxide (GO) sheets. When graphite is oxidized to GO, the individual graphene sheets become soluble in water and may be completely exfoliated using sonication.[16] The dispersions of GO sheets in water may then be simply deposited to produce large-area, few-monolayer films.[12] The resulting film microstructure is composed of many overlapping platelets since the lateral sheet dimensions average one micrometer after the oxidation[17] and exfoliation[16] process. Interestingly, on macro length scales this same microstructure for GO "paper"[18] exhibits superior mechanical properties to similar sp^2 carbon-based foils, and as we will show with additional chemical modification the mechanical properties of films can be further improved when extended to nanoscale dimensions. Indeed, we find that suspended GO-based membranes not only exhibit a high Young's moduli but also show quality factors comparable to diamond resonators. In the following letter, we present a practical and reproducible route to fabricate large-area, ultrathin GO films while maintaining mechanical properties approaching that of nominally pure graphene. We believe this process will facilitate a wafer-scale approach to forming NEMS-based devices from ultra stiff sp^2-bonded carbon materials.

Briefly, the film deposition process begins by centrifuging exfoliated GO platelets from water, isolating and resuspending the wet solids in methanol, and then using this solution to deposit films on SiO_2/Si substrates by a modified spin-casting technique (Figure 1a; Supporting Information). We find that accelerating solution evaporation by blowing dry nitrogen while spin-casting results in continuous films with GO platelets laying flat on the surface (Figure 1b). To promote binding between GO platelets water is driven off by a combination of low temperature thermal annealing and

* To whom correspondence should be addressed. E-mail: jeremy.robinson@nrl.navy.mil.
† Naval Research Laboratory.
‡ SFA Inc.

10.1021/nl8023092 CCC: $40.75
Published on Web 09/10/2008

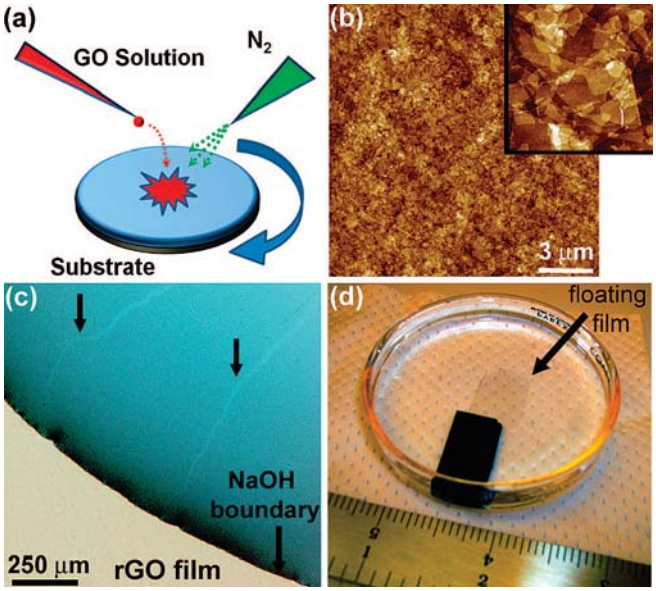

Figure 1. (a) Cartoon of the modified spin-coating technique. (b) Atomic force microscope (AFM) height image of a continuous graphene oxide (GO) film with an average thickness of 2 nm and roughness of 1 nm ($z = 6$ nm; inset image is 2.75×2.75 μm^2). (c) Optical microscope image demonstrating the release of a 4 nm thick reduced graphene oxide (rGO) film using sodium hydroxide. Arrows highlight two cracks forming in the delaminating film as the droplet propagates across the surface. (d) Digital picture of a rGO film transferred intact into water. The film is approximately 8 nm thick with lateral dimensions the same as the parent substrate (12×25 mm^2), which is submerged on the bottom of the Petri dish.

chemical reduction in a hydrazine hydrate vapor to form reduced graphene oxide (rGO).[12,16,19] After reduction, selective film delamination from the parent SiO_2 substrate is achieved by exposing films to a basic solution of sodium hydroxide (Figure 1c; Supporting Information). When subsequently dipped into water the entire delaminated film floats to the surface (Figure 1d) while regions of the film unexposed to the basic solution remain attached to the substrate.

Importantly, the controlled deposition, delamination, and transfer of rGO films opens the door to numerous mechanical[7,20,21] and nanoelectromechanical experiments.[6,22] Most notably, when films are recaptured and dried in air on textured substrates they are suspendable above the surface. Figure 2a,b shows an example of a 20 and 4 nm thick rGO film which has been suspended on a bed of Si pillars, formed through a chemical nanomachining process,[23] and extends hundreds of micrometers. We find by allowing an escape route for water during the drying process that we can consistently suspend films over areas as large as 0.5×0.5 mm, which is currently limited only by the extent of the support structure. To more easily extract the elastic properties of these rGO films, we created drum resonators by transferring films onto prepatterned, 250 nm SiO_2/Si substrates with holes etched through the oxide and ranging in diameter from 2.75 to 7.25 μm. Drying the rGO film over a field of holes typically results in three final configurations: the film is pulled into the hole and contacts the bottom (Supporting Information), the film spans the hole but ruptures presumably due to water escaping, or the film spans the hole intact (Figure 2c,d) and traps water beneath it. In the present work, we released the trapped water by using a focused ion beam (FIB) to mill a small hole ($<\sim$300 nm) in the centers of the membranes (Figure 2e). We note that the size and position of this hole has a minimal effect on the fundamental drum acoustics (Supporting Information).

To probe the elastic properties of these suspended rGO drum resonators, we use the well-established technique of

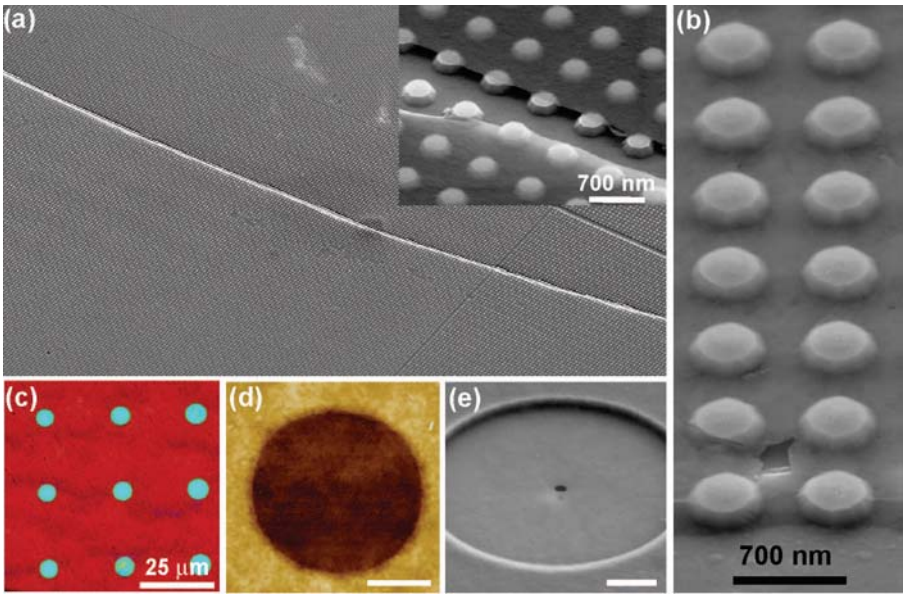

Figure 2. Transfer and drying of rGO films in air on prepatterned substrates. Scanning microscope (SEM) images show a (a) 20 nm and (b) 4 nm thick rGO film suspended on a bed of Si pillars (pillar height = 100 nm). The inset in (a) shows a magnified image of the crack in the film that runs diagonally across the field. In (b) a small rupture in the electron transparent film can be observed near the pattern edge. (c) Optical microscope image showing 9 rGO drum resonators. (d) AFM height image showing an intact drum resonator (thickness = 10 nm). The film is depressed approximately 10 nm below the top SiO_2 surface. (e) SEM image taken after a small hole was milled through a drum resonator (thickness = 15 nm). (Scale bar in panels d and e is 1 μm).

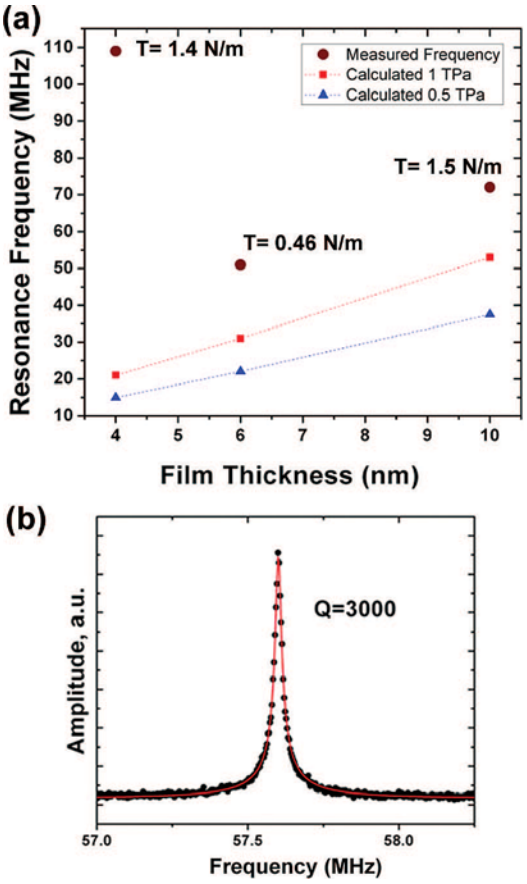

Figure 3. (a) Fundamental resonance frequency versus film thickness for rGO drum resonators (diameter = 2.75 μm). The theoretical values for a flat circular plate with E = 1 TPa (red squares) and 0.5 TPa (blue triangle) are also shown. Assuming membrane behavior, the tension (T) for each resonator is calculated. (b) Frequency versus amplitude curve for the 6 nm thick drum resonator shown in panel a demonstrating a Q-value of 3000.

laser interferometry (Supporting Information).[6,24] Briefly, a blue (412 nm) diode laser is used to thermoelastically modulate the rGO drums into resonance, while a red (633 nm) HeNe laser interferometrically measures the frequency of vibration in a Fabry−Pérot configuration. The fundamental frequency of vibration and overtone spacings can be affected by the tension (T) in the drum which can act either as a plate ($T \approx 0$) or as a membrane ($T > 0$). Determination of Young's modulus (E) is straightforward when the drum responds in the plate mode. For a circular plate the frequency modes are given by[25]

$$f_{mn} = \frac{\pi h}{4a^2}\sqrt{\frac{E}{3\rho(1-s^2)}}(\beta_{mn})^2 \quad (1)$$

where h is the film thickness, a is the drum radius, ρ is the material density, s is Poisson's ratio, and β_{nm} is the n^{th} root of the m^{th}-order Bessel function. When under high tension the circular drum frequencies follow a membrane behavior given by[25]

$$f_{mn} = \frac{1}{2a}\sqrt{\frac{T}{\rho h}}\beta_{mn} \quad (2)$$

Figure 3a shows the measured values for the fundamental resonance frequency of a 4, 6, and 10 nm thick rGO membrane. For all thicknesses, f_o is significantly higher than the calculated fundamental mode of a relaxed plate (eq 1), assuming a Young's modulus as reported for graphene (E = 0.5 TPa[26] or 1 TPa[6]), and suggests the drums are under tension (Figure 3a). Built-in tension has been observed for graphene resonators[6] and often results from the fabrication process. Fortuitously, this built-in tension together with enhanced adhesion to the SiO_2 substrate from remnant oxygen groups notably improves their quality factors (Q) over pure graphene resonators. Graphene resonators typically have Q-values of 10 to 200,[6] whereas our rGO resonators consistently show quality factors over 1500 (Figure 3b) with 4000 the highest value measured to date. These values compare favorably with state-of-the-art diamond resonators which typically have Q-values of ~3000 at room temperature.[27,28]

Though the tension enhances the mechanical response of the resonators, extracting the Young's modulus requires its removal, which we accomplished through thermal annealing. Figure 4a,b shows f_o versus drum diameter for a 15 nm thick film after annealing in argon at different temperatures for at least one hour. As described below after annealing at 300 °C the membranes are in the limit of zero tension. When membranes are annealed at successively higher temperatures f_o monotonically decreases as tension is released (Figure 4a and b), with the highest starting value at 5.3 N/m (Supporting Information). Note that annealing not only results in a drop of f_o but also a narrowing of the frequency distribution as resonators converge to zero tension.

Between approximately 240 and 260 °C, the release of built-in tension results in the originally flat membranes forming large-scale (>500 nm) corrugations as shown in Figure 4e,f. Interestingly, this wrinkling not only results in a transition in the f_o versus temperature curves (Figure 4b), but also the Q-value versus hole diameter curves (Figure 4c). Tension release in this manner indicates that resonator relaxation does not primarily occur through uniform platelet slipping since this would result in a flat structure. Rather, it appears that either localized regions of the membrane surface slip causing nonuniform tension and buckling, or that film adhesion at the drum rim is compromised and delaminates. This latter interpretation is supported by the observation that the slight Q-value versus hole diameter dependence disappears after wrinkle formation at 260 °C (Figure 4c) and the fact that hydrogen bonding to SiO_2 can be broken starting around 200 °C.[29]

After annealing at 300 °C, the suspended membranes are in the limit of zero tension allowing extraction of Young's modulus from the frequency response. Figure 4a shows frequency data for a series of the same resonators after annealing, along with the theoretical calculations for a flat circular plate (eq 1) with E = 0.5 and 1 TPa. Due to the resonator deformation after tension release, the frequency response deviates enough from the flat plate approximation

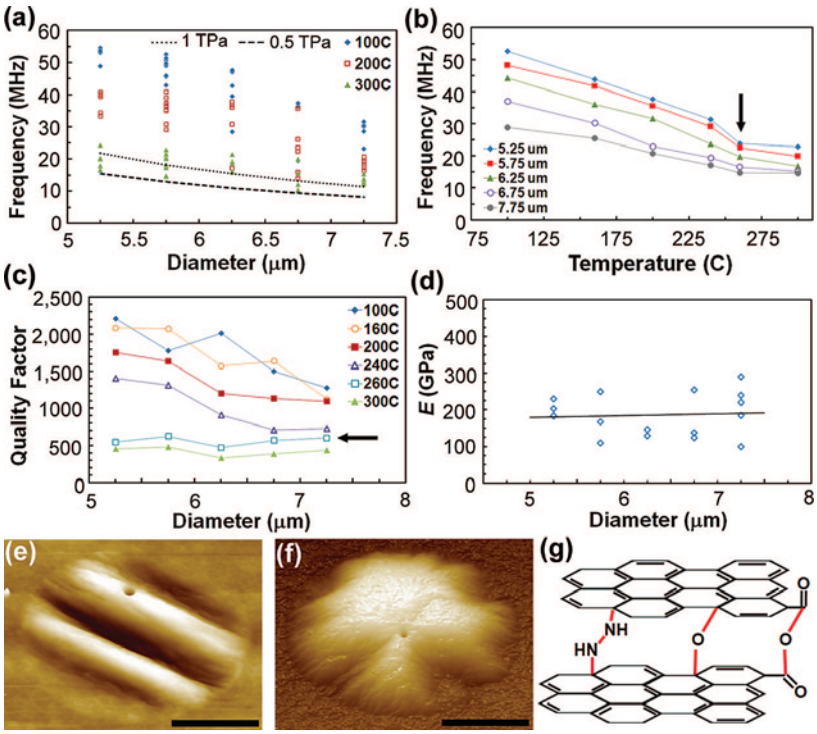

Figure 4. (a) The fundamental resonance frequency (f_o) vs drum diameter (D) for a series of rGO drums after thermal annealing. (b) Average f_o vs temperature for differently sized resonators (total = 53). (c) The average quality factors vs drum diameter. The arrows in panels b and c highlight when the membranes predominantly form wrinkles. (d) Extracted Young's modulus from FEM calculations vs hole diameter. (e,f) Perspective AFM images showing two corrugated states after thermal annealing (scale bar = 2 μm; Δz_{max} = 80 and 125 nm, respectively). The maximum ratio for out-of-plane deformation to drum diameter is ~1:45 (or 2%). (g) Schematic showing three covalent cross-links between rGO platelets.

such that finite element modeling (FEM) is necessary to more accurately extract E (Supporting Information). Figure 4d shows the FEM results after modeling 16 textured drums and reveals the modulus averages 185 GPa with a standard deviation of 58 GPa. This value is close to that recently reported for single, isolated GO sheets reduced via hydrogen plasma[30] and is several times higher than that found in macroscopic GO paper.[18]

This high Young's modulus for rGO films raises questions regarding the balance between the intraplatelet stiffness and interplatelet shear forces. The average lateral dimensions of a single GO platelet here measures approximately 1 μm, which means multiple overlapping sheets are necessary to span the 2.75 to 7.25 μm gaps. Even so, the frequency response demonstrates that Young's modulus is primarily dictated by the intraplatelet elastic response as opposed to the presumably weaker platelet-platelet interactions. We note it has been predicted that even a small addition of oxygen can significantly stiffen graphene sheets,[31] and this is likely adding to the mechanical rigidity.

Upon hydrazine reduction, oxygen is at least partially removed and some of the aromatic double-bonded carbons are recovered[12,16] however, reduction is never complete[16,32] enabling hydrogen bonding between individual rGO platelets. We suggest the hydrazine reduction chemistry[16] also leads to covalent cross-linking between neighboring platelets (Figure 4g), similar to GO paper with divalent ions,[33] due to the fact that these films remain intact in water (Figure 1d), withstand high in-plane tension, and show reduced frictional losses (i.e., Q-values similar to diamond). This suggestion could be tested in the future by, for example, detailed spectroscopic studies. Thus, tuning the interplatelet chemistry should allow further enhancement the mechanical properties of graphene oxide-based materials.

In conclusion, we have presented a manufacturable approach to producing ultrathin graphene-based materials for high-frequency nanomechanical devices. The controllable formation of graphene oxide films and subsequent chemical reduction restores the mechanical properties approaching that of graphene and allows the straightforward manipulation and transfer of films. The solution-based transfer process results in built-in tension and the highest reported quality factors for graphene resonators to date. Through thermal annealing the frequency response of suspended membranes can be systematically tuned via tension release, allowing identification of the Young's modulus for rGO thin films at 185 GPa. Finally, these results point to the exciting opportunities from chemically modifying sp^2-bonded carbon to form hybrid sp^2-sp^3 bonded materials that exhibit both strength and processability for nanoelectromechanical systems.

Acknowledgment. We thank D. Park and K. Bussmann for assistance with resonator fabrication. This research was at least partially performed while J.T.R and Z.W. held a National Research Council Research Associateship Award at the Naval Research Laboratory. J.T.R. fabricated the Si

pillar array at Lawrence Berkeley National Laboratory which was supported in part by the Director, Office of Science, Office of Basic Energy Sciences, Division of Materials Sciences and Engineering, of the U.S. Department of Energy under Contract No. DE-AC02-05CH11231. This work was supported in part by the Office of Naval Research.

Supporting Information Available: This material is available free of charge via the Internet at http://pubs.acs.org.

References

(1) Craighead, H. G. *Science* **2000**, *290* (5496), 1532–1535.
(2) Yang, Y. T.; Callegari, C.; Feng, X. L.; Ekinci, K. L.; Roukes, M. L. *Nano Lett.* **2006**, *6* (4), 583–586.
(3) Cleland, A. N.; Roukes, M. L. *Nature* **1998**, *392* (6672), 160–162.
(4) LaHaye, M. D.; Buu, O.; Camarota, B.; Schwab, K. C. *Science* **2004**, *304* (5667), 74–77.
(5) Freeman, M.; Hiebert, W. *Nat. Nanotechnol.* **2008**, *3* (5), 251–252.
(6) Bunch, J. S.; van der Zande, A. M.; Verbridge, S. S.; Frank, I. W.; Tanenbaum, D. M.; Parpia, J. M.; Craighead, H. G.; McEuen, P. L. *Science* **2007**, *315* (5811), 490–493.
(7) Frank, I. W.; Tanenbaum, D. M.; van der Zande, A. M.; McEuen, P. L. *J. Vac. Sci. Technol., B* **2007**, *256*, 2558–2561.
(8) Geim, A. K.; Novoselov, K. S. *Nat. Mater.* **2007**, *6* (3), 183–191.
(9) Novoselov, K. S.; Geim, A. K.; Morozov, S. V.; Jiang, D.; Zhang, Y.; Dubonos, S. V.; Grigorieva, I. V.; Firsov, A. A. *Science* **2004**, *306* (5696), 666–669.
(10) Novoselov, K. S.; Jiang, D.; Schedin, F.; Booth, T.; Khotkevich, V. V.; Morozov, S. V.; Geim, A. K. *Proc. Natl. Acad. Sci. U.S.A.* **2005**, *102*, 10451.
(11) Van Bommel, A. J.; Crombeen, J. E.; Van Tooren, A. *Surf. Sci.* **1975**, *48* (2), 463–472.
(12) Eda, G.; Fanchini, G.; Chhowalla, M. *Nat. Nanotechnol.* **2008**, . advanced online publication.
(13) Blake, P.; Brimicombe, P. D.; Nair, R. R.; Booth, T. J.; Jiang, D.; Schedin, F.; Ponomarenko, L. A.; Morozov, S. V.; Gleeson, H. F.; Hill, E. W.; Geim, A. K.; Novoselov, K. S. *Nano Lett.* **2008**, *8* (6), 1704–1708.
(14) Becerril, H.; Mao, J.; Liu, Z.; Stoltenberg, R. M.; Bao, Z.; Chen, Y. *ACS Nano* **2008**, *2* (3), 463–470.
(15) Wang, X.; Zhi, L.; Mullen, K. *Nano Lett.* **2008**, *8* (1), 323–327.
(16) Stankovich, S.; Dikin, D. A.; Piner, R. D.; Kohlhaas, K. A.; Kleinhammes, A.; Jia, Y.; Wu, Y.; Nguyen, S. T.; Ruoff, R. S. *Carbon* **2007**, *45* (7), 1558–1565.
(17) Li, J.-L.; Kudin, K. N.; McAllister, M. J.; Prud'homme, R. K.; Aksay, I. A.; Car, R. *Phys. Rev. Lett.* **2006**, *96* (17), 176101–4.
(18) Dikin, D. A.; Stankovich, S.; Zimney, E. J.; Piner, R. D.; Dommett, G. H. B.; Evmenenko, G.; Nguyen, S. T.; Ruoff, R. S. *Nature* **2007**, *448* (7152), 457–460.
(19) Gilje, S.; Han, S.; Wang, M.; Wang, K. L.; Kaner, R. B. *Nano Lett.* **2007**, *7* (11), 3394–3398.
(20) Huang, J.; Juszkiewicz, M.; de Jeu, W. H.; Cerda, E.; Emrick, T.; Menon, N.; Russell, T. P. *Science* **2007**, *317* (5838), 650–653.
(21) Poot, M.; van der Zant, H. S. J. *Appl. Phys. Lett.* **2008**, *92* (6), 063111−3.
(22) Zalalutdinov, M. K.; Baldwin, J. W.; Marcus, M. H.; Reichenbach, R. B.; Parpia, J. M.; Houston, B. H. *Appl. Phys. Lett.* **2006**, *88* (14), 143504–3.
(23) Robinson, J. T.; Evans, P. G.; Liddle, J. A.; Dubon, O. D. *Nano Lett.* **2007**, *7* (7), 2009–2013.
(24) Bak, J. H.; Kim, Y. D.; Hong, S. S.; Lee, B. Y.; Lee, S. R.; Jang, J. H.; Kim, M.; Char, K.; Hong, S.; Park, Y. D. *Nat. Mater.* **2008**, *7* (6), 459–463.
(25) Blevins, R. D. *Formulas for Natural Frequency and Mode Shape*; Krieger Publishing Company: Malabar, FL, 1979; pp 226, 240.
(26) Frank, I. W.; Tanenbaum, D. M.; van der Zande, A. M.; McEuen, P. L. In *Mechanical properties of suspended graphene sheets*; AVS: 2007; pp 2558−2561.
(27) Sekaric, L.; Parpia, J. M.; Craighead, H. G.; Feygelson, T.; Houston, B. H.; Butler, J. E. *Appl. Phys. Lett.* **2002**, *81* (23), 4455–4457.
(28) Hutchinson, A. B.; Truitt, P. A.; Schwab, K. C.; Sekaric, L.; Parpia, J. M.; Craighead, H. G.; Butler, J. E. *Appl. Phys. Lett.* **2004**, *84* (6), 972–974.
(29) Pierce, D. E.; Murray, R. A.; Lareau, R.; Laffey, S.; Vig, J. R. In *Outgassing of Quartz, IEEE International Frequency Control Symposium*, 1994; pp 107–114.
(30) Gomez-Navarro, C.; Burghard, M.; Kern, K. *Nano Lett.* **2008**,
(31) Incze, A.; Pasturel, A.; Peyla, P. *Phys. Rev. B* **2004**, *70*, 212103.
(32) Li, D.; Muller, M. B.; Gilje, S.; Kaner, R. B.; Wallace, G. G. *Nat. Nanotechnol.* **2008**, *3* (2), 101–105.
(33) Park, S.; Lee, K.-S.; Bozoklu, G.; Cai, W.; Nguyen, S. T.; Ruoff, R. S. *ACS Nano* **2008**, *2* (3), 572–578.

NL8023092